Review

A Review of Noble Metal Catalysts for Catalytic Removal of VOCs

Shaoqi Chu [1,2], Enlai Wang [1], Fushan Feng [1], Changsheng Zhang [2], Jie Jiang [2], Qinqin Zhang [3] , Fang Wang [1], Liancheng Bing [1], Guangjian Wang [1] and Dezhi Han [1,*]

[1]   State Key Laboratory Base of Eco-Chemical Engineering, College of Chemical Engineering, Qingdao University of Science and Technology, Qingdao 266042, China
[2]   SINOPEC Research Institute of Safety Engineering Co., Ltd., Qingdao 266000, China
[3]   Shandong Provincial Key Laboratory of Biochemical Engineering, College of Marine Science and Biological Engineering, Qingdao University of Science and Technology, Qingdao 266042, China
*   Correspondence: handzh@qust.edu.cn

Abstract: Volatile organic compounds (VOCs) are important precursors for the formation of secondary pollutants, such as fine particulate matter (PM) and ozone (O_3), which will lead to severe atmospheric environmental problems to restrict the sustainable development of the social economy. Catalytic oxidation is a safe, eco-friendly, and simple method for eliminating VOCs, which can be converted into CO_2 and H_2O without the generation of other harmful substances. The fabrication and development of catalysts are very crucial to enhance the catalytic oxidation efficiency of the removal of VOCs. The noble metal catalyst is one of the commonly used catalysts for the catalytic oxidation of VOCs because of the high reaction activity, good stability, poisoning-resistant ability, and easy regeneration. In this review, the research progress of noble metal (Pt, Pd, Au, Ag, and Ir) catalysts for the removal of VOCs in recent years was summarized with the discussion of the influence factors in the preparation process on the catalytic performance. The reaction mechanisms of the removal of VOCs over the corresponding noble metal catalysts were also briefly discussed.

Keywords: volatile organic compounds; catalytic oxidation; noble metal catalyst; reaction mechanism; support

1. Introduction

With the fast development of the economy, society, and industry in recent years, environmental pollution has become an increasingly serious issue, such as the emission of particulate matter (PM), automobile/industrial exhaust gas, industrial sewage, etc. [1–5] Particularly, volatile organic compounds (VOCs) exhibit the characteristics of a pungent odor, toxicity, and carcinogenicity, which will result in a severe threat to the ecological system and human health (Table 1) [6,7]. As shown in Figure 1, the emission of VOCs from China's petroleum industry increased by 24.08% from the year 2013 to 2019, which is much higher than that (4.07%) of the chemical industry [8,9]. Presently, there are some problems in the VOCs treatment technology, such as imperfect regulations and standards, inadequate environmental supervision, inefficient catalysts and processes, etc.

Generally, the effective methods to deal with VOCs are classified as membrane separation, adsorption, direct incineration, catalytic oxidation, etc. The membrane separation technology is one of the effective methods to remove low-concentration VOCs, which has been verified in the removal of formaldehyde (HCHO), benzene, n-hexane, and other VOCs [10]. However, the high cost, low stability, and low flux of separation membranes hinder its wide application in industry. Adsorption is also one of the common methods to remove VOCs, which may require the pretreatment of malodorants or the pre-removal of moisture. For example, Xiang et al. employed hickory wood to prepare biochar for adsorbing the VOCs [11]. The adsorption efficiency could be limited by the porosity of

most traditional adsorbents. The direct incineration method is used to burn the VOCs at high temperatures (800–1400 °C), which is especially used to deal with the VOCs for poisoning the catalyst. The removal rate of VOCs in the modern incineration system can reach 95–99%, while the conversion of halogenated compounds may need additional control equipment [12–14].

Table 1. Effects of some VOCs on the environment and human health [7].

Pollutants	Effect on the Environment	Effect on the Human	Source of Emission
Formaldehyde	Indoor air pollution	Skin allergy, nasopharynx discomfort, cough, acute and chronic bronchitis, and other respiratory diseases	Incomplete combustion of interior decoration, fuel, and tobacco
Benzene	Water and air pollution and photochemical smog	Long-term inhalation will damage the nervous system of people, and acute poisoning will cause nervous spasm, even coma, and death	Gases volatilized from automobile exhaust, paint, adhesives, and furniture
Toluene	Water and air pollution	Problems while pregnancy: retardation, premature delivery, congenital malformations	Volatilization of perfume, detergent, wallpaper, adhesive, paint, and burning of tobacco
Acetone	Strong ecological toxicity, water and air pollution	Adverse effects on the nervous system	Burning waste materials, the exhaust of automobiles, tobacco smoke, landfills
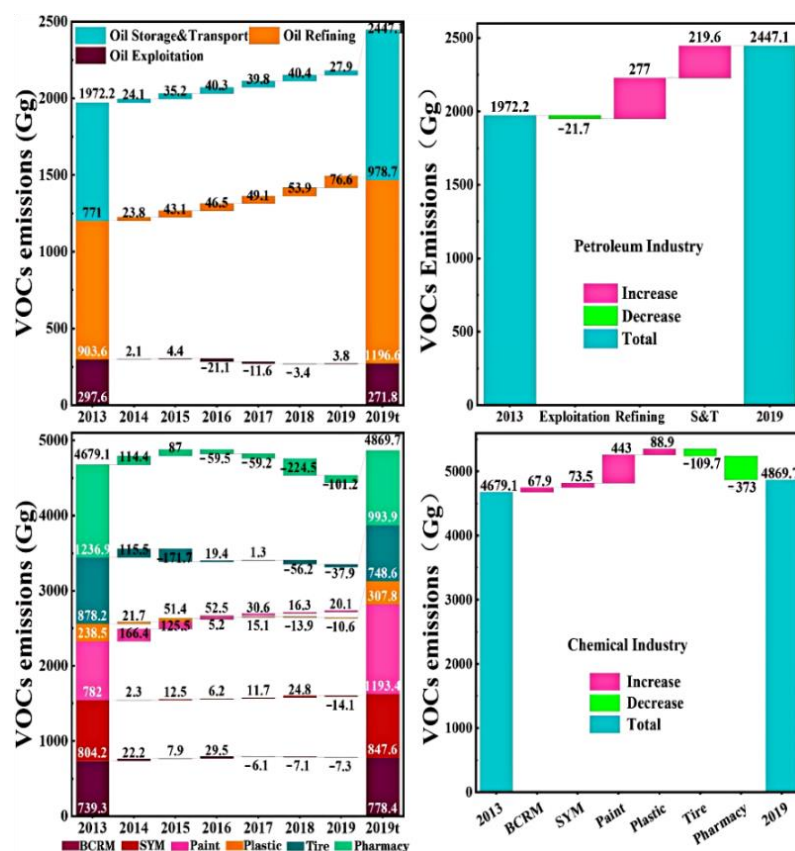
Figure 1. Time variation trend of emissions of VOCs from China's petroleum and chemical industries from 2013 to 2019 [8].

Alternatively, the catalytic oxidation process (COP) can effectively treat VOCs at a low temperature with low emissions of toxic and harmful byproducts, in which the catalysts do

not require a frequent regeneration [15]. The metal materials such as Pt, Pd, Ni, Cu, etc., were used as the catalysts, while air, oxygen, ozone, etc., were employed as the oxidants in the COP [16]. Except for the intensive application for the treatment of VOCs, the COP also is used to deal with oxygen-containing organic gas, sewage treatment, automobile exhaust, and so on [17,18]. One of the classic applications of the noble metal catalysts for the catalytic oxidation of VOCs is the three-way catalysts in the automotive industry, CO, NO_x, and hydrocarbons, and other harmful substances are produced due to the insufficient combustion of fuel. Ternary catalysts usually contain Pt, Pd, Rh, and other noble metals to convert the emitted hydrocarbons into CO_2 and H_2O. Thus, the emitted vehicle exhaust becomes clean, and its negative impact on the environment and human health is reduced. Because engine emissions sometimes occur during a cold start, the improvement on the catalytic activity of noble metal catalysts at low temperatures has become a common concern of academia and industry [5,19–21]. Not only in the automobile industry but also in chemical and other industries, noble metal catalytic oxidation catalysts are also widely used.

The design, optimization, and preparation of catalysts are the key steps for enhancing their catalytic performance in COP. Catalytic oxidation catalysts are generally divided into noble metal catalysts and non-noble metal oxide catalysts, which can completely oxidize hydrocarbons to H_2O and CO_2 under relatively mild conditions [22]. Although the preparation cost of non-noble metal catalysts is cheap, their poisoning-resistant ability and stability are relatively low compared with those of noble metal catalysts [23,24]. The noble metal catalysts exhibited many advantages, such as a high activity at a low temperature, a good stability, and an easy regeneration and storage [22]. Moreover, some noble metal catalysts could be prepared under mild synthesis conditions via the simple synthesis methods, while the preparation cost of noble metal catalysts is relatively high. Therefore, the utilization efficiency of noble metal active components should be improved to reduce the preparation cost of noble metal catalysts.

Some previous reviews of the catalytic oxidation of VOCs summarized the removal mechanism of VOCs, the intrinsic properties of noble metal active sites and supports, catalyst deactivation mechanism, etc. [16,25,26]. The noble metal (Pt, Pd, Au, Ag, Ir, etc.) supported catalysts can achieve the complete oxidation of VOCs at lower temperatures [27–30]. Many factors can influence the catalytic oxidation performance of the obtained noble metal type catalyst, including the preparation methods, the physicochemical properties of the support and additives, and the size and chemical state of the noble metal [31–35]. In this review, the reaction mechanisms and the influence factors in the preparation process for the Pt-based and Pd-based catalysts are discussed firstly, and the other noble metal (Au, Ag, and Ir) catalysts are also briefly introduced.

2. Pt-Based Catalysts

2.1. Reaction Mechanism of VOCs over Pt-Based Catalysts

The investigation of the reaction mechanisms of VOCs is particularly important for the design of high-performance Pt-based catalysts [36–38]. However, it is still difficult to provide a universal and unique reaction mechanism due to the different properties of VOCs under various reaction conditions. For instance, in the catalytic oxidation of toluene over the Pt/CeO_2 catalyst, the CeO_2 support could facilitate the dispersion of Pt species and promote the adsorption and activation of oxygen at the active sites [39]. Thus, the toluene was catalytically oxidized through the Langmuir Hinshelwood (L-H) kinetic model as follows, toluene → benzyl alcohol → benzaldehyde → benzoic acid → CO_2 and H_2O. Wen et al. prepared the meso-Pt/CeO_2 catalyst with an ordered mesoporous structure for the catalytic oxidation of toluene (Figure 2) [40]. The toluene molecules were firstly adsorbed on the surface metal active centers and oxygen vacancies of the prepared catalyst. Then, the surface-active oxygen interacted with the C–H bond of the methyl group to form the benzyl group, and subsequently produce benzyl alcohol. The benzyl alcohol was further

oxidized by the remaining active oxygen to intermediate products, such as benzoic acid, benzoate, and maleic anhydride, which finally were oxidized into CO_2 and H_2O.
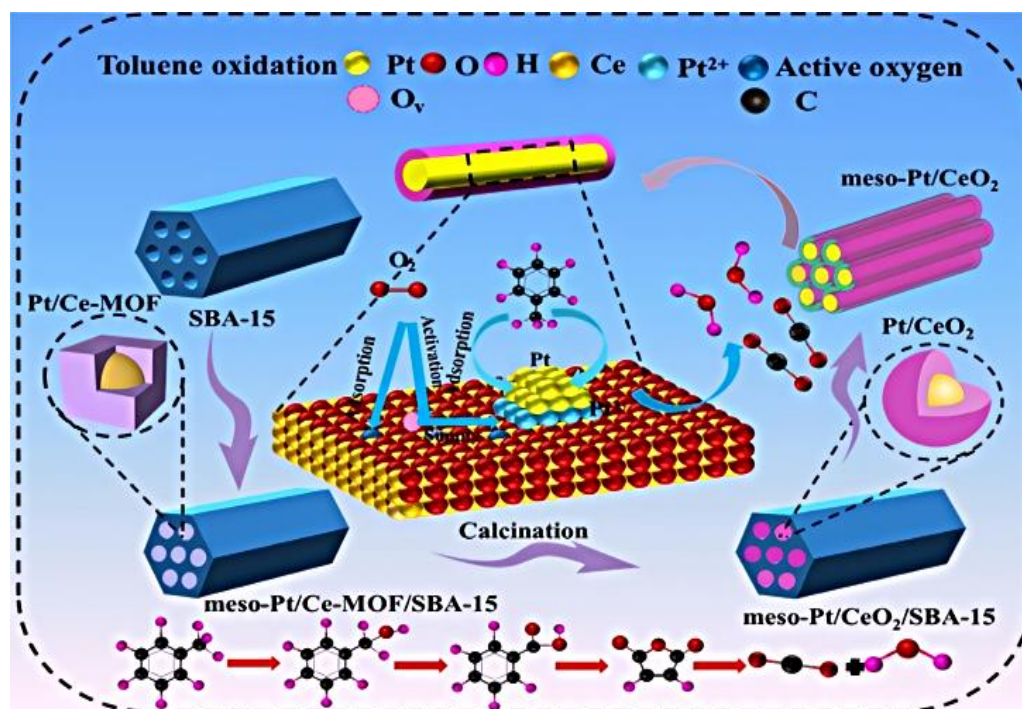

Figure 2. The possible reaction pathway and mechanism on meso-Pt/CeO$_2$ Catalyst [40].

Wang et al. prepared the Pt/TiO$_2$ catalyst by the impregnation method for the catalytic oxidation of toluene [41]. When the reaction temperature was low, the disproportionation reaction of adsorbed toluene occurred to produce benzene and p-xylene. Additionally, then o-xylene was formed by the isomerization of p-xylene. The oxygen-containing intermediates with the benzene ring, such as benzyl alcohol, benzaldehyde, and benzoic acid, may be formed by the sequential oxidation of chemically adsorbed toluene molecules by surface active oxygen. On the other hand, the oxidation of o-xylene is most likely to form phthalic acid. With the increase in the reaction temperature, the phthalic acid and benzoic acid can be further oxidized to maleic anhydride and itaconic anhydride, which were transformed to the small acetone and acetic acid by a ring-opening reaction, respectively. Finally, these small molecules are completely oxidized to CO_2 and H_2O (Figure 3).

Wang et al. studied the oxidation mechanism of a mixed VOCs system over the Pt/TiO$_2$ catalyst [42], revealing that the oxidation of mixed components did not generate new intermediates compared with the oxidation of single-component toluene or acetone (Figure 4). However, the research on the reaction mechanism of a mixed VOCs system still needs to be further explored.

In addition, in the case of the catalytic oxidation of HCHO, room temperature catalytic decomposition is considered to be the main method to continuously and effectively eliminate indoor HCHO [43]. Ye et al. proposed the possible oxidation mechanism of HCHO over the prepared Pt/Co$_3$O$_4$-NiO catalyst (Figure 5) [43]. They believed that HCHO was first converted into the intermediate species dioxymethylene (DOM), which was converted into formate. The formate species was finally decomposed into CO_2 and H_2O. In this process, the oxidation of DOM to formate was faster than the decomposition of formate, thus the decomposition of the formate species became the rate control step of the complete oxidation reaction of HCHO.
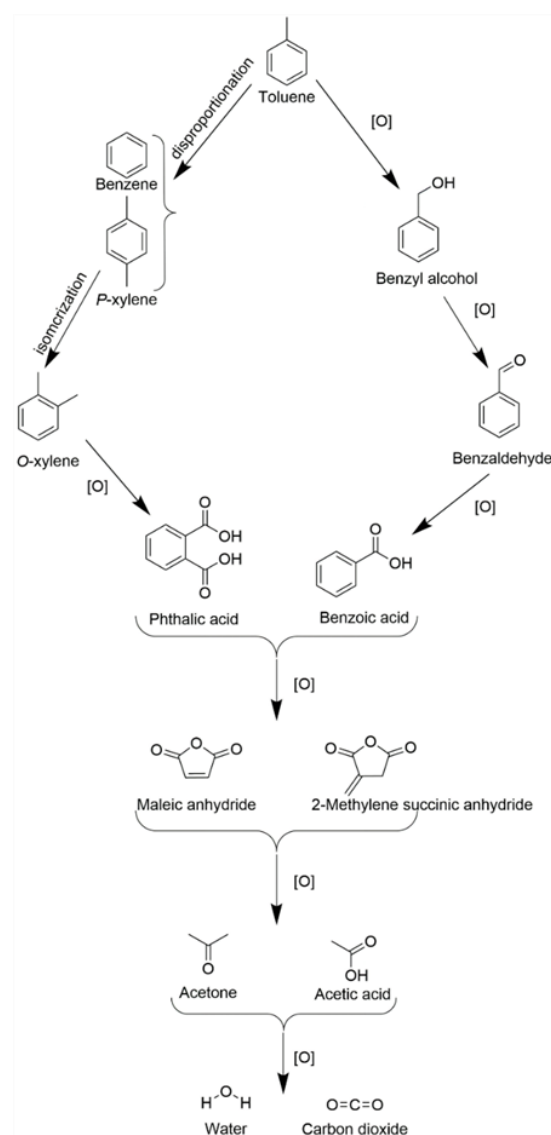
Figure 3. The possible catalytic mechanism for toluene oxidation over 0.2 wt% Pt/TiO$_2$ [41].

Zhang et al. proposed almost the same oxidation path for HCHO over noble metal catalysts using TiO$_2$ as the support [44]. Additionally, the activity of the Pt-based catalyst was higher than that of other metal (Rh, Pd, and Au) catalysts.

2.2. Influence of Preparation Method

The interaction between the active component and the support is one of the key factors affecting the activity of the prepared catalysts, which is mainly subjected to the catalyst preparation methods.

Kondratowicz et al. prepared two different catalysts (Pt-I/@Zr and Pt-G/@Zr) for the catalytic oxidation of toluene, acetone, n-hexane, and other VOCs by the traditional wet impregnation and ethylene glycol reduction deposition methods, respectively [45]. The second approach was based on an introduction of metallic Pt nanoparticles prepared in the polyol process. The catalyst (Pt-G/@Zr) prepared by the ethylene glycol reduction deposition method has a better catalytic performance than the Pt-I/@Zr catalyst. When the average conversion rate of VOCs reached 90%, the reaction temperature of Pt-G/@Zr was about 100 °C lower than that (279 °C) of Pt-I/@Zr. It was found that Pt nanoparticles were mainly distributed on the outer surface of ZrO$_2$ to form large particles over the Pt-G/@Zr catalyst. However, in the preparation of the Pt-I/@Zr catalyst by the traditional

wet impregnation process, the Pt^{4+} cations were impregnated into the pores of the ZrO_2 support, covering part of the active sites in the pores of the carrier, resulting in the low utilization efficiency of the active sites, and thus the low reaction activity of the obtained catalyst (Figure 6). Therefore, it necessary to develop the efficient preparation methods to tune the dispersion and location of the Pt active sites of the obtained catalysts in the COP of VOCs.
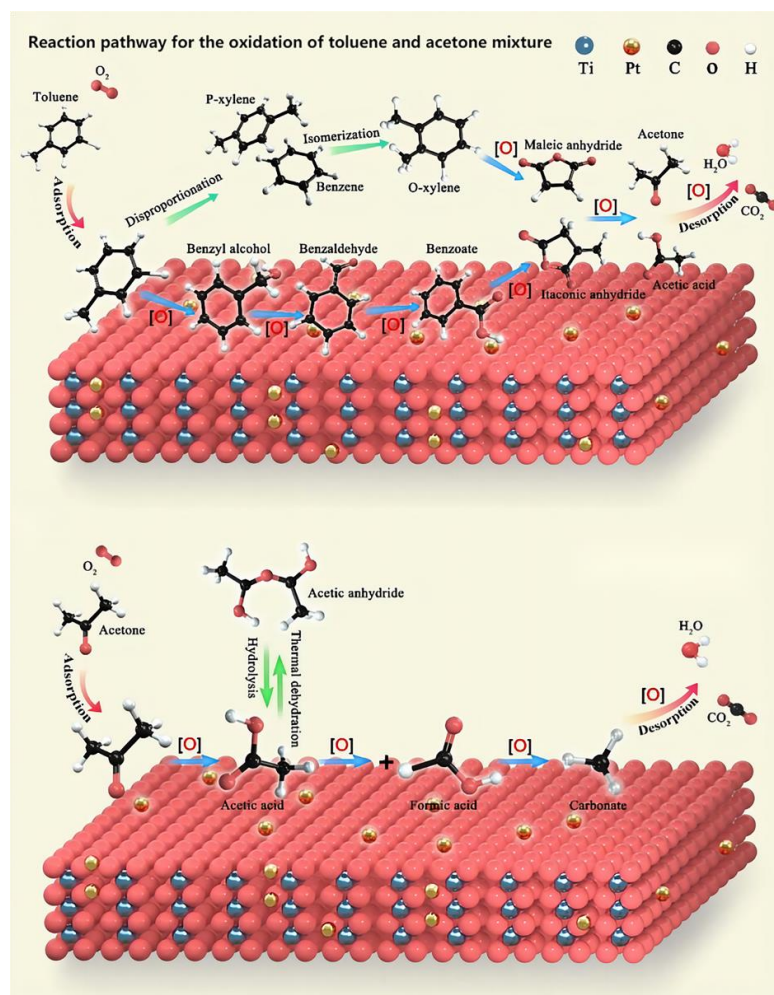

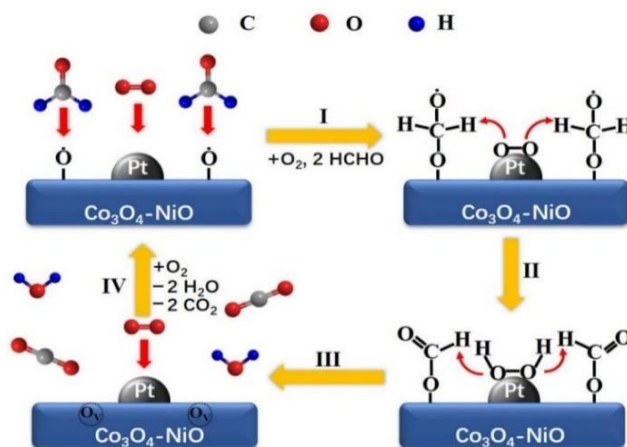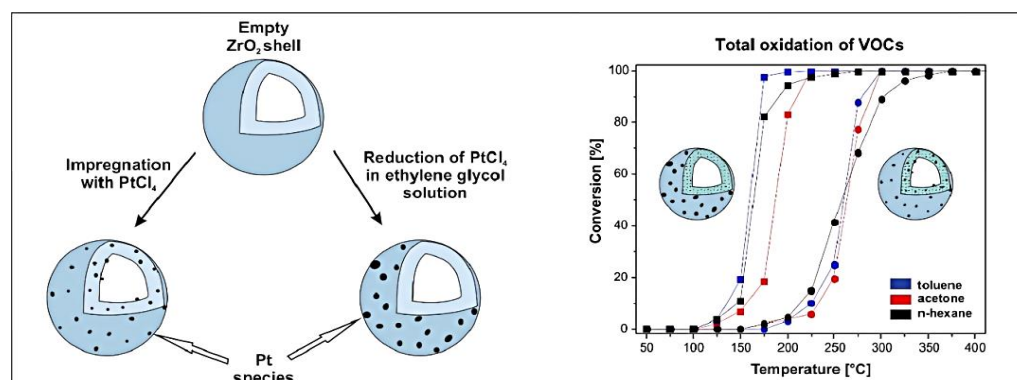**Figure 4.** Mixed reaction path of toluene and acetone over Pt/TiO_2 catalyst [42].

Figure 5. HCHO oxidation mechanism on Pt/Co_3O_4-NiO catalyst [43].

Figure 6. Pt particle distribution of catalysts prepared by different methods (**left**) and different VOCs removal effects (**right**) [45].

An et al. prepared a series of Pt/Fe_2O_3 catalytic oxidation catalysts for the low-temperature oxidation of HCHO using the impregnation method, coprecipitation method, and colloidal deposition method, respectively [35]. Among these catalysts, the Pt/Fe_2O_3-CD catalyst prepared by colloidal deposition exhibited the highest activity for the oxidation of HCHO due to the high dispersion of the Pt species (Figure 7), which could weaken the Fe–O bond nearby, enhance the migration rate of the active oxygen, and promote the adsorption and activation of the oxygen to participate in the oxidation of HCHO. Pt colloidal solution can be obtained via the colloid deposition method by adding NaOH into the Pt precursor solution, followed by mixing with the carrier, filtering, washing, and a calcination to prepare the final catalyst.
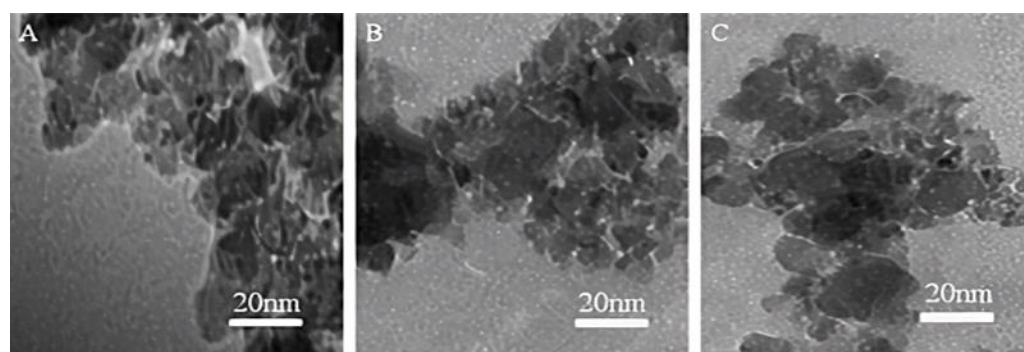
Figure 7. TEM image of (**A**) Pt/Fe_2O_3-CD, (**B**) Pt/Fe_2O_3-CP, (**C**) Pt/Fe_2O_3-IMP (Pt particles are dark dots in the figure) [35].

2.3. Influence of Chemical Valence of Pt

The chemical valence of Pt is one of the important factors affecting the catalytic activity of Pt-based catalysts for COP of VOCs. An et al. prepared supported Pt catalysts by the impregnation method using three silica materials, namely gas phase SiO_2 (f-SiO_2), porous particle SiO_2 (g-SiO_2), and mesoporous SBA-15, for the catalytic oxidation of HCHO [46]. It is found that the Pt/f-SiO_2 catalyst exhibited the highest activity with a 100% conversion of HCHO at room temperature, which was much lower than that of 50 and 110 °C over the Pt/SBA-15 and Pt/g-SiO_2, respectively. This is due to the high proportion of Pt^0 in the Pt/f-SiO_2 catalyst according to the analysis of the XPS results (Table 2). The appropriate proportion of Pt^0/Pt^{2+} is the key factor to improve the catalytic ability of the prepared catalyst for activating oxygen molecules at a low temperature. A similar result was also reported by Kim et al. in the study of the effect of a H_2 high-temperature (300 °C) reduction in the catalytic performance of the Pt/TiO_2 catalyst for the oxidation of gaseous benzene [47]. The analysis of the XPS results indicated that the content of the Pt^0 particles in the Pt/TiO_2-R catalyst with a H_2 reduction was about 2.8 times higher than that of the Pt/TiO_2 catalyst

without a H_2 reduction (Figure 8). Correspondingly, the Pt/TiO$_2$-R catalyst possessed the high conversion (90%) of gaseous benzene at 167 °C.

Table 2. Summary of XPS data of three catalysts for HCHO oxidation [46].

Catalyst	Binding Energy Pt 4f$_{7/2}$ (eV)		Pt^0/(Pt^0 + Pt^{2+})
	Pt^0	Pt^{2+}	
Pt/f-SiO$_2$	71.2	72.6	0.48
Pt/SBA-15	71.4	72.4	0.33
Pt/g-SiO$_2$	71.4	72.5	0.30
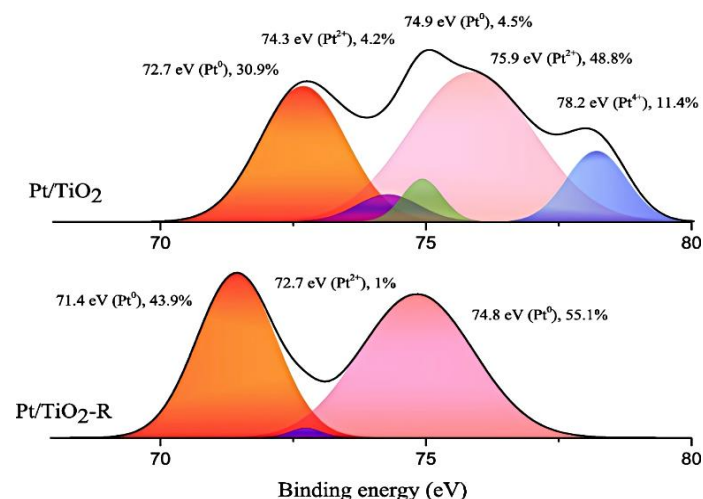
Figure 8. XPS spectra of Pt/TiO$_2$ without H$_2$ reduction and Pt/TiO$_2$-R with H$_2$ reduction [47].

2.4. Influence of the Support Type

For Pt-based catalysts, the catalyst activity is closely related to the types of support. Peng et al. prepared Pt-based catalysts by using CeO$_2$ nanorods (CeO$_2$-r), CeO$_2$ nanoparticles (CeO$_2$-p), and CeO$_2$ nanocubes (CeO$_2$-c), respectively [48]. When the toluene conversion was 90%, the reaction temperature of CeO$_2$-r was only 150 °C, which was much lower than that of 175 °C and 190 °C of CeO$_2$-p and CeO$_2$-c, respectively.

Avila et al. prepared Pt-based catalysts with CeO$_2$, TiO$_2$, and Al$_2$O$_3$ as the support, respectively, for the catalytic oxidation of propylene and propane [49]. The order of activity over the three catalysts in the propane oxidation is Pt/TiO$_2$ > Pt/CeO$_2$ > Pt/Al$_2$O$_3$. It was found that the propane oxidation occurred not only at the Pt^0 site but also at the Pt^0-Ce^{3+} site, which provides a new way for the propane oxidation reaction. In addition, the propane adsorption capacity of Pt/TiO$_2$ is 5.5 times that of Pt/CeO$_2$, which is the reason for the high catalytic activity of the Pt/TiO$_2$ catalyst. In the case of a propylene oxidation, the reaction order of propylene is negative, while the reaction order of oxygen is positive, proving that propylene is easier to form an adsorption state than oxygen in the propylene oxidation reaction. The Pt/CeO$_2$ catalyst with the best propylene oxidation performance could provide more oxygen vacancies to accelerate the reaction rate.

2.5. Influence of Pt Particle Size

The conversion of some VOCs is sensitive to the Pt particle size of the prepared Pt-based catalysts [33,34,50].

Zeolite is considered to be one of the excellent supports for loading active components due to its large specific surface area and unique pore structure [51–54]. Khawaja et al. prepared the Pt/NaY catalysts using modified Y zeolite through three steps: dealumination, desiliconization, and an acid treatment [55]. The characterization results demonstrated that the Pt-NaY$_{mod}$ catalyst with a mesoporous structure exhibited a higher activity in the catalytic oxidation of toluene than the Pt-NaY catalyst with only a pure microporous

structure, which is due to the reduced Pt particle size in the NaY_{mod} catalyst (Figure 9). Moreover, the existence of mesopores in the prepared NaY_{mod} catalyst also had the positive effect on the reduction in the catalyst carbon's deposition and the improvement in the catalyst's stability.
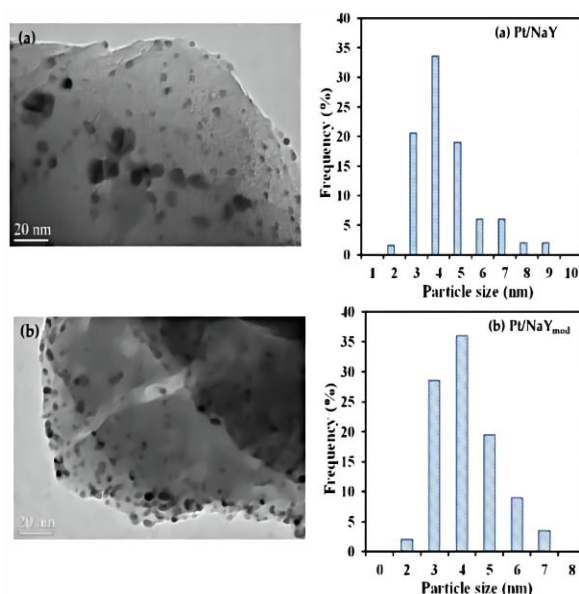
Figure 9. TEM images and size distribution of (**a**) Pt/NaY, (**b**) Pt/NaY_{mod} [55].

Wang et al. employed different zeolites (ZSM-5, S-1, Beta, and USY) as supports to prepare Pt-based catalysts with a micro-/meso-porous composite structure through an organic alkali TPAOH treatment [32]. The results showed that the Pt/ZSM-5 catalyst with a high dispersion and small particle size (ds = 3.5 nm) had a low $T_{90\%}$ of 130, 150, 210, and 180 °C for the conversion of benzene, n-hexane, acetonitrile, and ethyl acetate, respectively (Figure 10).
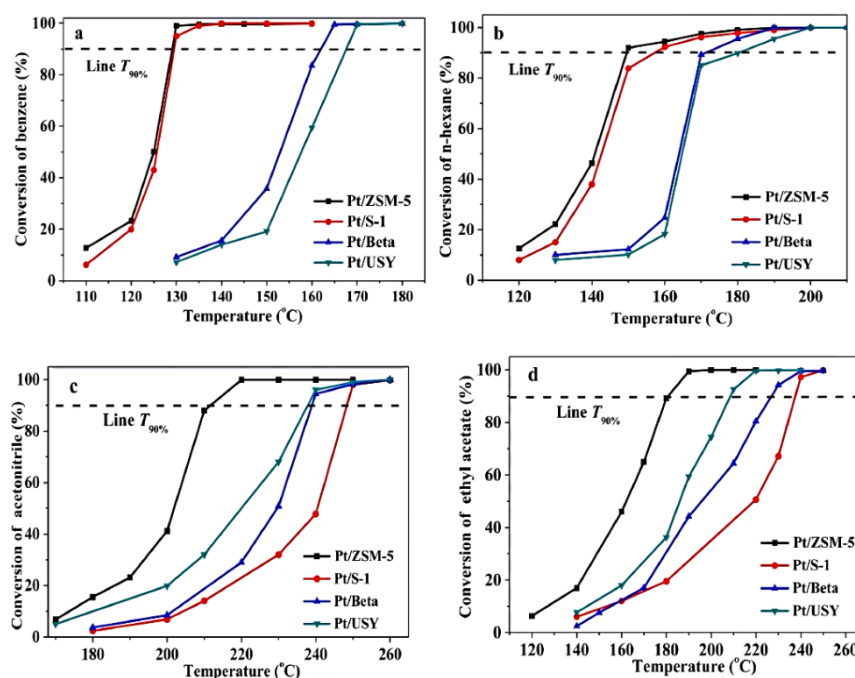
Figure 10. The catalytic activity of (**a**) benzene, (**b**) n-hexane, (**c**) acetonitrile, and (**d**) ethyl acetate oxidation over the Pt/zeolite catalysts. $T_{90\%}$: temperature corresponding to reactant conversion = 90% [32].

Huang et al. synthesized a series of Pt/TiO_2 catalysts with different Pt particle sizes [56]. It was found that the obtained catalyst with a Pt particle size of about 10 nm exhibited a superior catalytic performance in the oxidation of HCHO (Figure 11).
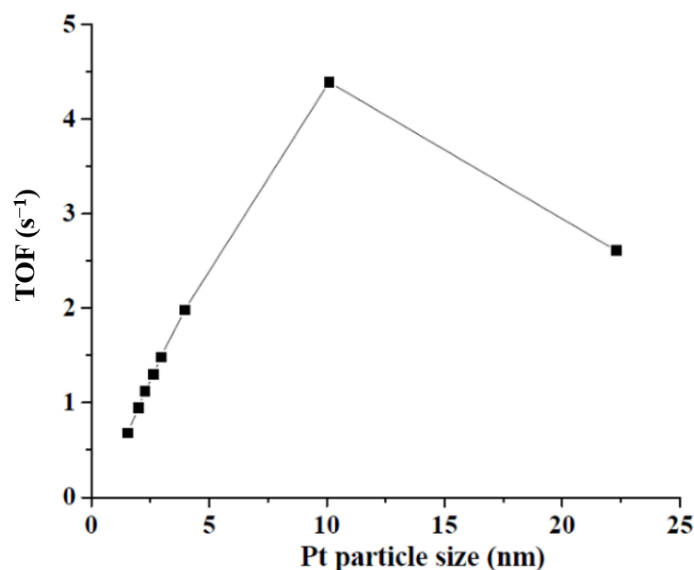

Figure 11. TOFs as a function of Pt particle size of Pt/TiO_2 catalyst for HCHO oxidation reaction [56].

The reaction conditions and activities of some Pt-based catalysts for the removal of VOCs were listed in Table 3.

Table 3. Pt-based catalysts for the removal of VOCs.

Catalyst	Type of VOCs	Content of VOCs (ppm)	T (°C)	Conversion (%)	Ref.
$Pt_{0.008}$-G/@Zr	C_7H_8	1000	172	90	[45]
$Pt_{0.002}/CeO_2$-r	C_7H_8	1000	150	90	[48]
$Pt_{0.005}$-NaY$_{mod}$	C_7H_8	1000	130	90	[55]
$Pt_{0.01}/TiO_2$-R	C_6H_6	100	167	90	[47]
$Pt_{0.005}/ZSM$-5	C_6H_6	1000	130	90	[32]
$Pt_{0.01}/TiO_2$-R-120	HCHO	40	25	81.3	[56]
$Pt_{0.01}/f$-SiO$_2$	HCHO	300	25	100	[46]
$Pt_{0.05}/CeO_2$	C_3H_6	8000	190	50	[49]
$Pt_{0.005}/TiO_2$	C_3H_8	8000	330	50	[49]

3. Pd-Based Catalysts

3.1. Reaction Mechanism of VOCs over Pd-Based Catalysts

In the reaction mechanism of the Pd-based catalyst, Wei et al. studied the catalytic oxidation of benzene on Pd particles in detail [57]. It was found that C_6H_6 was mainly dehydrogenated to C_6H through dehydrogenation oxidation (Figure 12a–f), and then was oxidized to C_6HO (Figure 12g), which was finally decomposed into smaller molecules (Figure 12h). In this process, the steps from C_6H_6 to C_6H_3 were the rate-controlling steps, and the C_6H_3O and C_6H_2O may be the important intermediates.
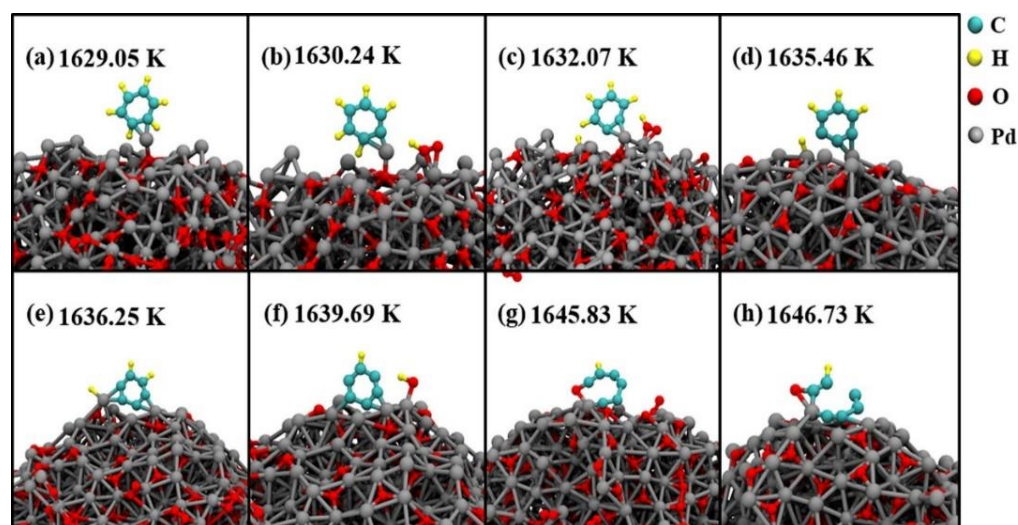
Figure 12. The oxidation process (**a**–**h**) of C_6H_6 on palladium nanoparticles [57].

Aguirre et al. believed that the catalytic oxidation of toluene over a Pd-based catalyst was similar to the Pt-based catalysts [58]. The toluene was dehydrogenated on the surface of the Pd/CeO$_2$ catalyst to form a benzyl species, and then gradually oxidized to benzyl alcohol (Figure 13). Subsequently, benzyl alcohol was further oxidized to the aldehyde species, then the formate species, which would generate the final CO$_2$ product. The conversion of the formate species to CO$_2$ was regarded as the rate control step of the whole reaction process. Additionally, the benzoic acid intermediates can also be oxidized to anhydride species (maleic anhydride or succinic anhydride), which accumulated on the catalyst surface to form CO$_2$ with a slow reaction rate.
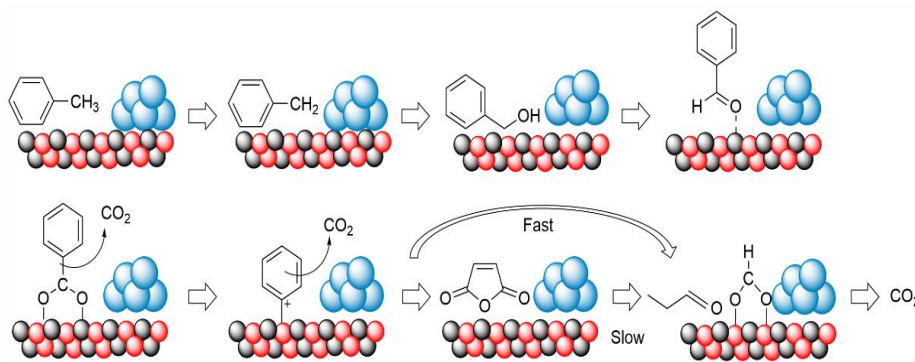
Figure 13. Mechanism of toluene oxidation on Pd/CeO$_2$ catalyst [58].

3.2. Influence of Acidity of the Supports

The acidity of the support would significantly influence the catalytic performance of the Pd-based catalysts in COP of VOCs. Compared with the neutral or basic support, Pd nanoparticles are easily oxidized on the acidic support because of their electrophilic properties to form electron-deficient Pd atoms [59,60].

Wu et al. believed that the high content of the medium-strength acidity of the support was one of the reasons for the high activity of the Pd/Silicalite-1-H catalyst in the oxidation of toluene [61]. Li et al. prepared Pd-based catalysts by using γ-Al$_2$O$_3$, ZSM-5, and SiO$_2$ for the oxidation of 1,2-dichlorobenzene [62]. The order of the activity of these catalysts was as follows: Pd/ZSM-5(25) > Pd/γ-Al$_2$O$_3$ > Pd/ZSM-5(200) > Pd/SiO$_2$. The Lewis (L) acid sites facilitated the adsorption of chlorinated organic molecules on the catalyst surface [63], while the Brønsted (B) acid could promote the breaking of C–C bonds and accelerate the oxidation reaction [64,65], which was responsible for the superior activity over the Pd/ZSM-5 (25) catalyst. (Figure 14 and Table 4).
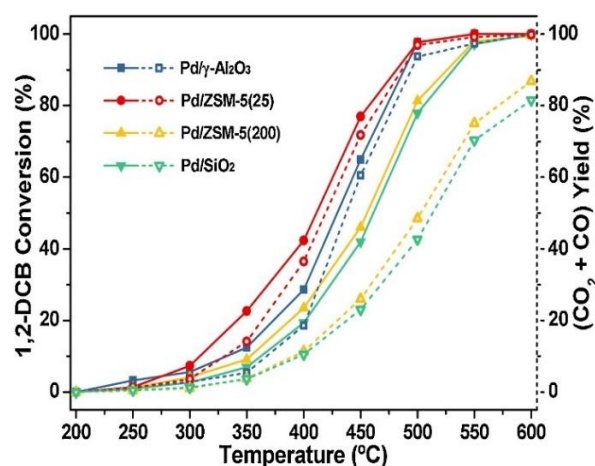
Figure 14. 1,2-dichlorobenzene conversion and selectivity of CO_2 and CO [62].

Table 4. Catalyst acidity measured by pyridine FT-IR [62].

Catalyst	Extremely Weak Acid		Weak Acid		Medium Strength Acid		Strong Acid	
	C_B	C_L	C_B	C_L	C_B	C_L	C_B	C_L
Pd/γ-Al$_2$O$_3$	–	0.54	-	0.31	-	0.19	-	0.12
Pd/ZSM-5 (25)	1.79	0.47	1.42	0.21	0.99	0.17	0.39	0.11
Pd/ZSM-5 (200)	0.17	0.28	0.09	0.05	0.08	0.04	-	-
Pd/SiO$_2$	–	0.19	-	0.01	-	-	-	-

C_B: concentration of B acid sites (mmol/g-cat.); C_L: concentration of L acid sites (mmol/g-cat.).

Jabłońska et al. prepared a series of Pd-based catalysts by using HY, NaY, and γ-Al$_2$O$_3$ as the support for the catalytic oxidation of methanol, demonstrating that the HY with an appropriate acidity could dramatically enhance the dispersion Pd species to promote the catalytic oxidation performance of the corresponding catalyst [66]. He et al. also believed that the acidity of the catalyst could promote the dispersion and oxidation of Pd particles, thus leading to the high activity of Pd/SBA-15 for the toluene oxidation reaction [67]. Deng et al. pretreated the ceramic and glass fiber with water, sulfuric acid, and nitric acid to fabricate the Pd-based catalysts for the catalytic oxidation of benzene [68]. The ceramic fiber with a relatively strong acidity facilitated the dispersion of the Pd particles, thus enhancing the efficiency of the benzene conversion.

However, Yue et al. found that the strong acid sites of the Pd/ZSM-5 catalyst would lead to the generation of more by-products during the catalytic oxidation of butyl acetate [69]. Additionally, the strong acidity may also lead to the carbon deposition for deactivating the catalyst, especially in the catalytic oxidation reaction of carbon-containing VOCs. Therefore, the regulation of the support acidity is critical for tuning the activity and stability of the catalysts in the removal of VOCs.

3.3. Influence of Support Type

Perovskite oxides are widely used as the catalyst support in the catalytic oxidation of VOCs due to their superior thermal stability and high oxygen migration rate. Yi et al. prepared the Pd-CeMnO$_3$ perovskite catalysts by the sol-gel method and impregnation method [70]. The high efficiency of benzene complete oxidation at 200 °C was achieved due to the high dispersion of Pd particles on the perovskite surface, and the enhanced interaction between Ce ions and Pd to accelerate the electron transfer for promoting the production of active oxygen.

He et al. prepared 3D@2D constructed Al$_2$O$_3$@CoMn$_2$O$_4$ microspheres to load the Pd nanoparticles for the catalytic oxidation of VOCs [71]. The obtained catalysts with the hollow hierarchical structure possessed the large specific surface area, more accessible active sites, and promoted the catalytic activity, especially the 1 wt% Pd/h-Al@4CoMn$_2$O$_4$

catalyst (the molar rate of Al and $CoMn_2O_4$: 4:1) with the best catalytic activity and high stability for the catalytic oxidation of VOCs (Figure 15).
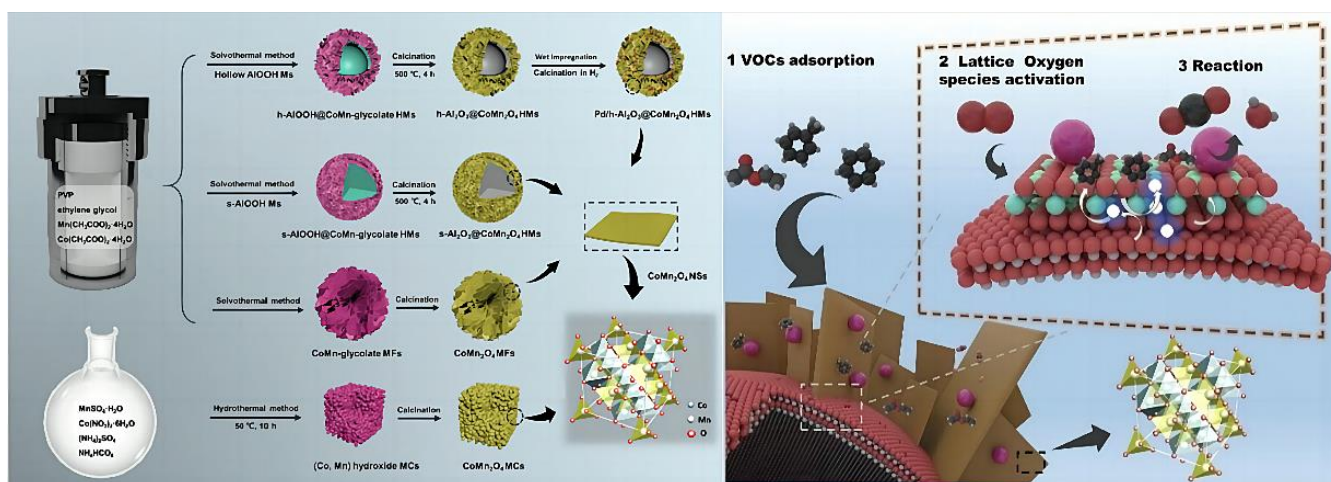
Figure 15. Schematic diagram of synthesis and structure of Pd/h-Al@$4CoMn_2O_4$ catalyst [71].

Moreover, the metal organic framework (MOF) is considered to be an excellent support to fabricate the Pd-based catalysts for the catalytic oxidation of VOCs [72]. Li et al. prepared the Pd/MOF catalysts by impregnating metal precursors in pre-fabricated MOFs (Figure 16) [73]. The obtained metal multifunctional organic compounds integrate a unique multifunctional organic structure to provide adsorption sites for VOCs, and highly dispersed metal nanoparticles provide a large number of catalytic active sites to efficiently catalyze the oxidation of VOCs.
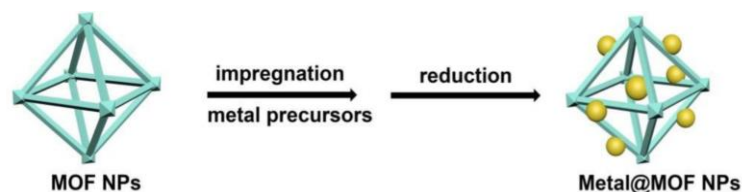

Figure 16. The schematic description of the preparation methods of metal/MOF NPs catalysts [73].

In recent years, single transition metal oxides, rare earth oxides, and mixed metal oxides have been employed as a catalyst support in the conversion of VOCs. The catalysts prepared with rare earth oxides as the support exhibited an excellent activity in the application of environmental catalysis [74]. For instance, the CeO_2 with abundant oxygen vacancies, a strong interaction with metals, and variable exposed crystal planes is one of the important catalyst supports in heterogeneous catalytic oxidation [75]. Gil et al. fabricated the Pd catalysts supported on CeO_2, TiO_2, and Al_2O_3, respectively, for the catalytic oxidation of propene [76]. It was found that the Pd metal had a stronger interaction with CeO_2 than other oxides, which was responsible for the enhanced catalytic oxidation activity.

3.4. Influence of Promoter

The catalyst promoter could generate the synergistic effect with the active component, change the active component–support interaction, and tune the acid property of the support for improving the catalyst activity in the catalytic removal of VOCs.

Zhao et al. prepared the Mn-modified Pd/TiO_2 catalyst by the simple impregnation method for the acetone oxidation reaction [77]. The high content of Pd^{2+}, abundant adsorbed oxygen, and low-temperature reducibility of $Pd_{0.01}Mn_{0.2}$/TiO_2 catalysts with a large particle size (d = 2.4 nm) could be responsible for the enhanced catalytic performance (Figure 17).
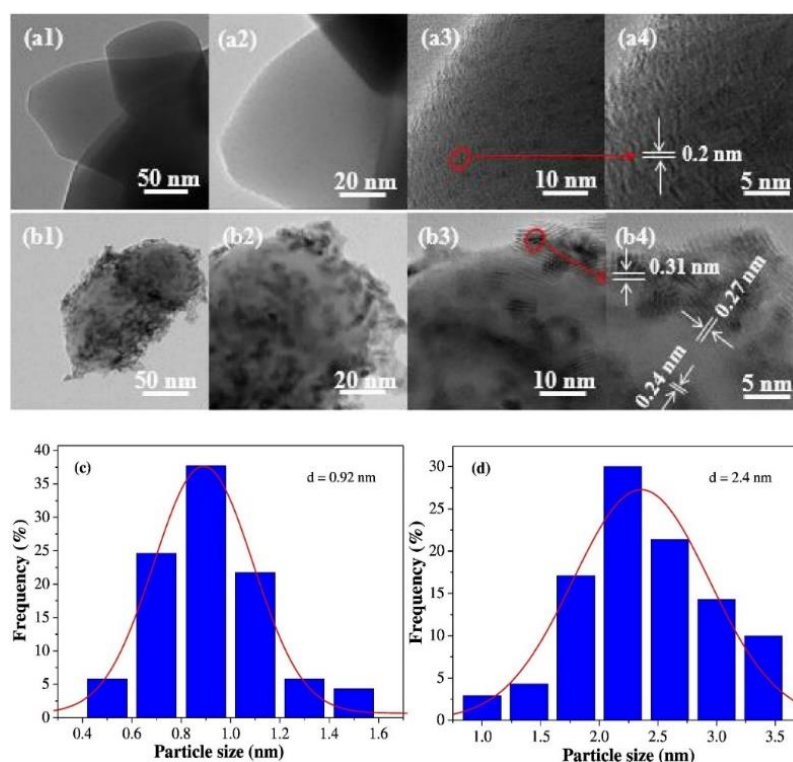
Figure 17. HRTEM results of (**a**,**c**) $Pd_{0.01}/TiO_2$ and (**b**,**d**) $Pd_{0.01}Mn_{0.2}/TiO_2$ catalysts for acetone oxidation reaction [77].

Similarly, Taylor et al. improved the activity of the Pd/TiO_2 catalyst by adding Nb with different loading amounts in the impregnation step of a catalyst preparation [78]. The propane oxidation activity of the prepared catalysts increased with the increase in the Nb loading amount due to the enhanced migration rate of oxygen. Gil et al. modified the Pd/Al_2O_3 catalyst by adding Fe, Ce, Ti, Mn, etc., for the catalytic oxidation of propylene [76]. The results showed that the addition of Ce and Fe improved the catalyst activity of the corresponding catalysts. Aznárez et al. also studied the effect of a Ce addition on the properties of the Pd/Al_2O_3 catalyst for the propylene conversion, indicating that the addition of Ce can effectively provide more strong acid sites of the prepared catalyst [79]. He et al. added the Mo promoter to the Pd/Al_2O_3 catalyst for the catalytic oxidation of benzene [80]. The addition of Mo could enhance the Pd dispersion (Figure 18), change the oxidation state of the Pd species, and promote the oxygen adsorption on the catalyst surface, thus effectively improving the activity and stability of the prepared Pd/Al_2O_3 catalyst.

The reaction conditions and activities of some Pd-based catalysts for the removal of VOCs were listed in Table 5.

Table 5. Pd-based catalysts for the removal of VOCs.

Catalyst	Type of VOCs	Content of VOCs (ppm)	T (°C)	Conversion (%)	Ref.
$Pd_{0.005}/SBA-15$	C_7H_8	1000	227	90	[67]
$Pd_{0.0028}/Silicalite-1-H$	C_7H_8	1000	189	90	[61]
$Pd_{0.05}/h-Al@4CoMn_2O_4$	C_7H_8	50	165	100	[71]
$Pd_{0.005}-CeMnO_3$	C_6H_6	500	200	100	[70]
$Pd_{0.01}-Mo_{0.05}/Al_2O_3$	C_6H_6	2000	190	90	[80]
Pd/CeO_2	C_3H_6	1000	213	80	[76]
$Pd_{0.005}-Nb_{0.06}/TiO_2$	C_3H_8	5000	370	90	[78]
$Pd_{0.005}-Ce_{0.01}/Al_2O_3$	C_3H_6	5000	303	90	[79]
$Pd_{0.01}Mn_{0.2}/TiO_2$	C_3H_6O	1000	259	95	[77]
$Pd_{0.015}/HY$	CH_3OH	40,000	120	90	[66]
$Pd_{0.005}/ZSM-5$ (25)	$C_6H_4Cl_2$	450	474	90	[62]
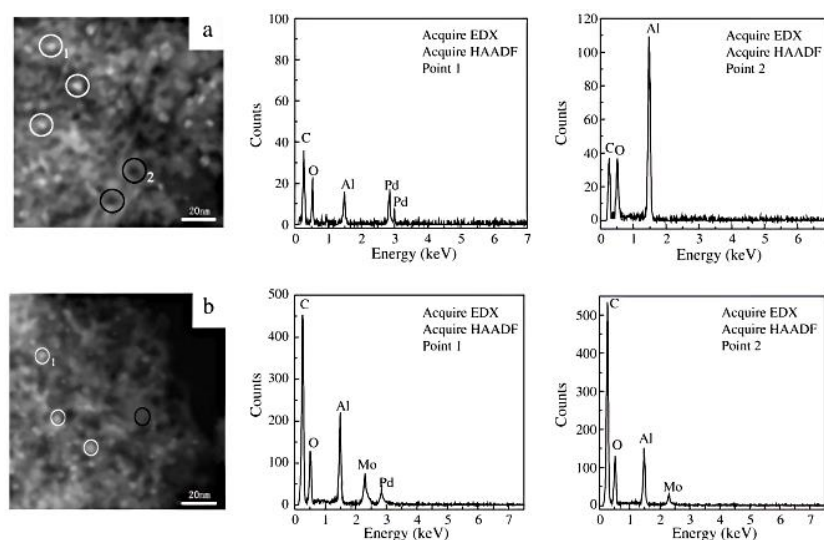
Figure 18. HAADF-STEM and EDS of $1.0\%Pd/Al_2O_3$ (**a**) and $1.0\%Pd$-$5\%Mo/Al_2O_3$ (**b**) catalyst [80].

4. Other Noble Metal Catalysts

4.1. Au-Based Catalysts

Au nanoparticles exhibit the unique performance in the catalytic oxidation of VOCs, which has attracted great interest from researchers [81,82]. Although the catalytic activity of Au-based catalysts is lower than that of Pt- and Pd-based catalysts, the highly dispersed Au on the oxide support with the high specific surface area can lead to the improved catalytic activity of the catalytic oxidation of VOCs, and the higher CO_2 selectivity in comparison with other noble-based catalysts [83]. The performance of Au-based catalysts for the catalytic oxidation of VOCs is highly dependent on the size of Au particles and the physicochemical characteristics of the supports, which are dramatically influenced by the preparation methods and pretreatment conditions [82,84,85].

Solsona et al. prepared a series of Au-based catalysts by three different methods (the coprecipitation method, deposition precipitation method, and impregnation method) for the catalytic oxidation of alkanes [86]. It was found that the Au/CoO_x catalyst prepared by the coprecipitation method was effective for the total combustion of propane with the reaction temperature of 200 °C, in which the Au could promote the reducibility of the support to increase the catalyst reactivity.

CeO_2, as an excellent oxygen storage material, is often used as the support for preparing Au-based catalysts. The CeO_2 can enhance the dispersion of Au particles with a small and stable particle size, leading to the elevated catalytic oxidation performance of the obtained Au-based catalysts. For instance, Jia et al. compared the catalytic oxidation activity of HCHO over the TiO_2 and CeO_2 supported Au catalysts, demonstrating that the Au/CeO_2 catalyst showed a higher activity with $T_{100\%}$ of 80 °C for the HCHO oxidation [87]. Shen et al. also prepared a set of Au/CeO_2 catalysts with a low Au content (≤ 0.85 wt%) and small Au crystals (<2–3 nm) by the coprecipitation method, revealing that the calcination temperature was crucial to achieving a highly dispersed gold species for an effective HCHO oxidation. The 0.78Au catalyst calcined at 300 °C could realize the complete oxidation of HCHO at only 107 °C (Figure 19) [88].

Therefore, the choice of suitable supports is very critical to realize the high dispersion of the Au species, thus improving the catalytic oxidation performance of the corresponding catalysts in the removal of VOCs. Moreover, the bimetallic catalysts containing Au particles usually exhibit a better catalytic performance than the single metal catalysts, which also has attracted interest from researchers recently [89,90]. For example, Hosseini et al. studied the catalytic performance of bimetallic Pd-Au catalysts deposited on a mesoporous TiO_2 support [91]. It was found that the Pd(shell)-Au(core)/TiO_2 catalyst possessed a higher

catalytic activity for the oxidation of toluene and propylene than that of the catalysts with the alloy or Au (shell)-Pd (core) morphology (Figure 20).
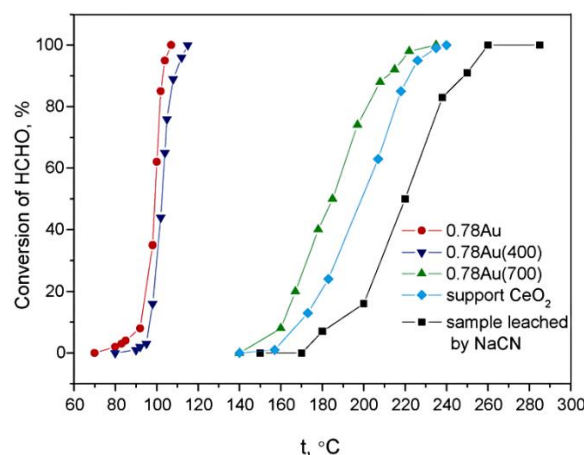

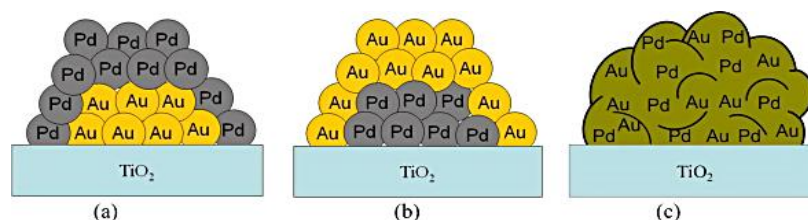**Figure 19.** Effect of calcination temperature on oxidation of HCHO over Au/CeO$_2$ catalyst [88].

Figure 20. (**a**) Pd(shell)-Au(core)/TiO$_2$; (**b**) Au(shell)-Pd(core)/TiO$_2$; (**c**) Pd-Au(alloy)/TiO$_2$ [91].

4.2. Ag-Based Catalysts

Compared to the Pt, Pd, and Au active metals, Ag is relatively cheap in the preparation of the catalysts for the removal of VOCs. Moreover, Ag could generate the synergistic effect with metal oxide supports, and enhance the formation of oxygen active species during the catalytic oxidation of VOCs, leading to the improved catalytic activity of the obtained catalysts [92]. The catalytic activity of Ag-based catalysts is closely related to the characteristics of the supports [93]. In recent years, transition metal oxides have attracted much attention due to their low price and acceptable catalytic activity [94–96].

Tang et al. prepared Ag-based catalysts supported by three different metal oxides for toluene oxidation [97]. The reaction activity order was Ag-Mn-O > Ag-Co-O > Ag-Ce-O. In addition, the Ag-Mn-O catalyst also showed a high stability at room temperature. Bhat et al. prepared the Ag/TiO$_2$ catalyst by encapsulating the Ag species in porous reducible TiO$_2$ support, demonstrating that the encapsulation method can prevent the sintering of the active metal Ag to improve the activity of the prepared catalyst compared with the traditional impregnation method [96].

In terms of the CeO$_2$ support, Wang et al. prepared a series of Ag/CeO$_2$ catalysts by different methods for the catalytic oxidation of toluene, indicating that the preparation methods had a great impact on the physicochemical properties of the fabricated Ag-based catalysts [93]. The catalyst (Ag-Ce-BTC-C) prepared by the one-pot solvothermal method exhibited the optimum performance due to the abundant active Ag species, more concentration of oxygen vacancies, and the large molar ratio of O$_{ads}$/O$_{lat}$, Ce^{3+}/Ce^{4+}, and Ag^0/Ag$^{\delta+}$ (Figure 21).
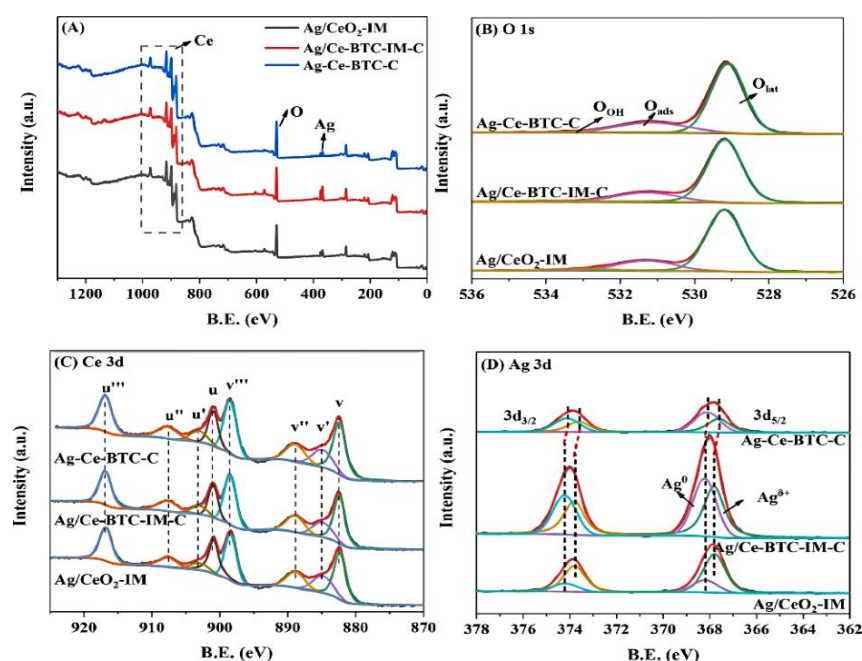
Figure 21. XPS spectra of the supported Ag catalysts: (**A**) full spectra, (**B**) O 1s, (**C**) Ce 3d, and (**D**) Ag 3d [93].

Benaissa et al. studied the influence of three preparation methods (impregnation reduction, urea precipitation, and wet impregnation) on the performance of the Ag/CeO_2 catalyst in the total oxidation of propylene [95]. Among these catalysts, the catalyst (Ag loading of 4 wt%) prepared by impregnation reduction exhibited the highest catalytic activity due to the presence of the Ag^{2+}, Ag^+, and Ag^0 species to allow an electronic interaction among the different redox couples.

Dong et al. employed the polyvinyl alcohol-protected reduction method to prepare the layered MnO_2-supported Ag catalysts with the reduced graphene oxide (rGO) as the promoter for the oxidation of ethyl acetate [94]. The $1.0Ag-1.0rGO/\delta-MnO_2$ catalyst showed a superior catalytic performance in ethyl acetate oxidation (E_a = 39.8 kJ/mol, $T_{90\%}$ = 160 °C), which is due to the enhanced interaction between Ag and MnO_2, high O_{ads}/O_{latt} molar ratio, and good low-temperature reducibility (Figure 22).
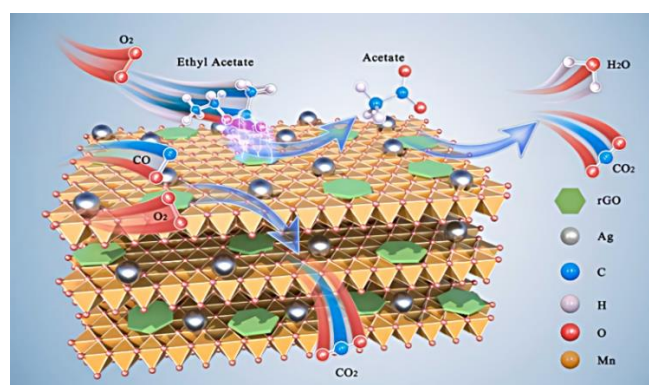

Figure 22. Oxidation model of ethyl acetate over $1.0Ag-1.0rGO/\delta-MnO_2$ catalyst [94].

4.3. Ir-Based Catalysts

Although the reaction rate of Ir-based catalysts is generally lower than that of commonly used Pt-based and Pd-based catalysts, they exhibit the high anti-sintering ability in the oxygen-containing atmosphere during the catalytic oxidation of VOCs [98,99].

Wang et al. fabricated the $Ir/Ce/Al_2O_3$ catalysts by confining the CeO_2 particles' size for the complete oxidation of toluene, in which the size of CeO_2 nanoparticles and loaded ultrafine Ir^0 nanoparticles was <5 nm and <2 nm, respectively (Figure 23) [100]. The strong IrO_2-CeO_2 interaction was responsible for the optimized $Ir^0/Ir^{\delta+}$ ratio in the H_2-reduced $Ir/Ce(A)/Al_2O_3$-H_2 catalyst (with the addition of acetic acid), resulting in the improvement of the catalyst activity with $T_{90\%}$ of 290 °C for the toluene conversion, which was lower than that of 306 and 318 °C over the H_2-reduced Ir/Al_2O_3-H_2 and $Ir/Ce(W)/Al_2O_3$-H_2 (without the addition of acetic acid), respectively.
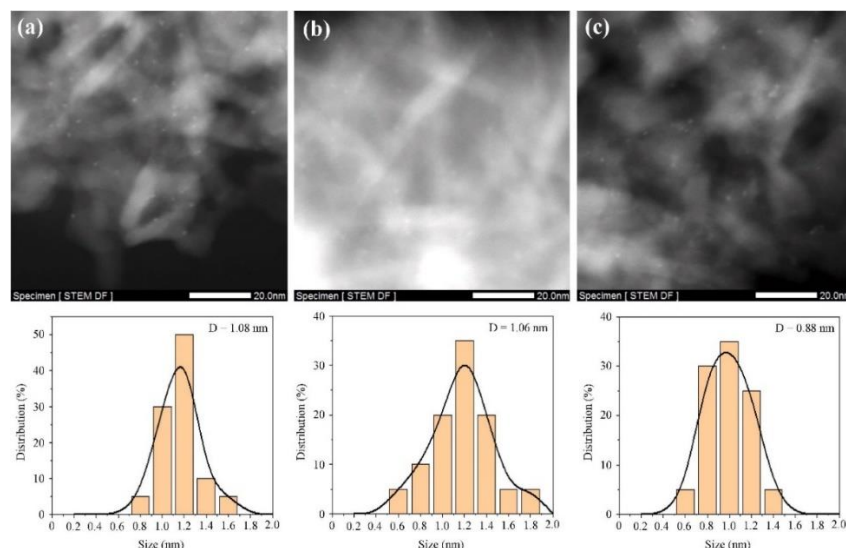
Figure 23. HAADF-STEM images and the corresponding particle size distribution of Ir: (**a**) Ir/Al_2O_3-H_2, (**b**) $Ir/Ce(W)/Al_2O_3$-H_2, and (**c**) $Ir/Ce(A)/Al_2O_3$-H_2 [100].

Schick et al. investigated the relationship between the Ir particle size and the total oxidation activity of short-chain alkanes over the Ir/SiO_2 catalysts [99]. The Ir particle size in the prepared catalysts could be tuned by changing the calcination temperature. A low-temperature calcination (350 °C) would facilitate the formation of small Ir particles (ca. 5 nm), leading to an increase in the defective Ir^{3+} species and a high proportion of highly reducible iridium species for enhancing the catalyst activity. The similar structure–performance relationship was also found in a methane oxidation over the Ir-based catalysts [99].

Thus, the activity of Ir-based catalysts for the catalytic oxidation of VOCs can be effectively improved by using appropriate supports and adjusting the structure and chemical state of Ir particles.

5. Conclusions and Prospect

To reduce the emission of VOCs, high-efficiency catalytic oxidation catalysts have been fabricated and developed with a high stability and poisoning-resistant ability in recent years. Noble metal catalysts, such as Pt-, Pd-, Au-, Ag-, Ir-, etc., based catalysts were intensively used in the removal of VOCs from industry and academia due to their advantages of a high activity, good stability, and easy regeneration. The catalytic performance of these catalysts is determined by many factors, for instance, the particle's size, dispersion degree, and the valence of noble metal as well as the metal-support interaction, etc. Therefore, many studies mainly focus on the effects of the types or properties of supports and metals, the catalyst preparation methods, and catalyst promoters on the catalytic performance during the removal of VOCs. Due to the high preparation cost of noble metal catalysts, it is also very important to reduce the loading amount of noble metal to prepare the catalysts with an acceptable activity and stability. The stability and lifetime of the noble metal catalysts should be further improved. Since most catalytic oxidation reactions for the removal of

VOCs are the oxidation of carbon-containing compounds at high temperatures, it is also very important to improve the anti-sintering and anti-carbon deposition properties of the catalysts. Moreover, the reaction and deactivation mechanism of the catalytic oxidation still need further investigation due to the complexity of the various catalysts and different VOCs. Additionally, the influence of the reaction conditions, such as the addition of water vapor or sulfide on the catalytic performance, can be further optimized in the subsequent studies. The regeneration and recycling of the deactivated catalysts were also critical to reduce the preparation and operation costs in the removal of VOCs.

Author Contributions: Conceptualization, S.C. and D.H.; methodology, C.Z.; writing—original draft preparation, S.C., E.W., and F.F.; writing—review and editing, D.H., Q.Z.; supervision, J.J.; project administration, G.W.; funding acquisition, D.H., F.W. and L.B.; All authors have read and agreed to the published version of the manuscript.

Data Availability Statement: Data sharing not applicable.

Conflicts of Interest: The authors declare no conflict of interest.

References

1. Dockery, D.W. Health effects of particulate air pollution. *Ann. Epidemiol.* **2009**, *19*, 257–263. [CrossRef]
2. Scalas, A.; Yoshida, N. Multiparty session types, beyond duality. *J. Log. Algebr. Methods* **2018**, *97*, 55–84. [CrossRef]
3. Cong, X. Air pollution from industrial waste gas emissions is associated with cancer incidences in Shanghai, China. *Environ. Sci. Pollut. Res. Int.* **2018**, *25*, 13067–13078. [CrossRef] [PubMed]
4. Geng, Y.; Wang, M.; Sarkis, J.; Xue, B.; Zhang, L.; Fujita, T.; Yu, X.; Ren, W.; Zhang, L.; Dong, H. Spatial-temporal patterns and driving factors for industrial wastewater emission in China. *J. Clean. Prod.* **2014**, *76*, 116–124. [CrossRef]
5. Sinha Majumdar, S.; Pihl, J.A. Impact of selected high-performance fuel blends on three-way catalyst light off under synthetic spark-ignition engine-exhaust conditions. *Energy Fuels* **2020**, *34*, 12900–12910. [CrossRef]
6. Harb, P.; Locoge, N.; Thevenet, F. Treatment of household product emissions in indoor air: Real scale assessment of the removal processes. *Chem. Eng. J.* **2020**, *380*, 122525. [CrossRef]
7. Soni, V.; Singh, P.; Shree, V.; Goel, V. Effects of VOCs on human health. *Air Pollut. Control* **2018**, 119–142. [CrossRef]
8. Simayi, M.; Shi, Y.; Xi, Z.; Ren, J.; Hini, G.; Xie, S. Emission trends of industrial VOCs in china since the clean air action and future reduction perspectives. *Sci. Total Environ.* **2022**, *826*, 153994. [CrossRef]
9. Kamal, M.S.; Razzak, S.A.; Hossain, M.M. Catalytic oxidation of volatile organic compounds (VOCs)—A review. *Atmos. Environ.* **2016**, *140*, 117–134. [CrossRef]
10. Aguado, S. Removal of pollutants from indoor air using zeolite membranes. *J. Membr. Sci* **2004**, *240*, 159–166. [CrossRef]
11. Xiang, W.; Zhang, X.; Chen, K.; Fang, J.; He, F.; Hu, X.; Tsang, D.C.W.; Ok, Y.S.; Gao, B. Enhanced adsorption performance and governing mechanisms of ball-milled biochar for the removal of volatile organic compounds (VOCs). *Chem. Eng. J.* **2020**, *385*, 123842. [CrossRef]
12. Ray, S.; Kim, K.H.; Yoon, H.O. Effect of incineration on the removal of key offensive odorants released from a landfill leachate treatment station (LLTS). *Chemosphere* **2012**, *87*, 557–565. [CrossRef] [PubMed]
13. Tomatis, M.; Moreira, M.T.; Xu, H.; Deng, W.; He, J.; Parvez, A.M. Removal of VOCs from waste gases using various thermal oxidizers: A comparative study based on life cycle assessment and cost analysis in China. *J. Clean. Prod.* **2019**, *233*, 808–818. [CrossRef]
14. Parmar, G.R.; Rao, N.N. Emerging control technologies for volatile organic compounds. *Crit. Rev. Environ. Sci. Technol.* **2008**, *39*, 41–78. [CrossRef]
15. Liotta, L.F. Catalytic oxidation of volatile organic compounds on supported noble metals. *Appl. Catal. B-Environ.* **2010**, *100*, 403–412. [CrossRef]
16. Huang, H.; Xu, Y.; Feng, Q.; Leung, D.Y.C. Leung. Low temperature catalytic oxidation of volatile organic compounds: A review. *Catal. Sci. Technol.* **2015**, *5*, 2649–2669. [CrossRef]
17. Wang, J.; Chen, H. Catalytic ozonation for water and wastewater treatment: Recent advances and perspective. *Sci. Total Environ.* **2020**, *704*, 135249. [CrossRef]
18. Twigg, M.V. Rôles of catalytic oxidation in control of vehicle exhaust emissions. *Catal. Today* **2006**, *117*, 407–418. [CrossRef]

19.	Sinha Majumdar, S.; Pihl, J.A.; Toops, T.J. Reactivity of novel high-performance fuels on commercial three-way catalysts for control of emissions from spark-ignition engines. *Appl. Energy* **2019**, *255*, 113640. [CrossRef]

20.	Kang, S.B.; Nam, S.B.; Cho, B.K.; Nam, I.-S.; Kim, C.H.; Oh, S.H. Effect of speciated HCs on the performance of modern commercial TWCs. *Catal. Today* **2014**, *231*, 3–14. [CrossRef]

21.	Diehl, F.; Barbier, J.; Duprez, D.; Guibard, I.; Mabilon, G. Catalytic oxidation of heavy hydrocarbons over Pt/Al$_2$O$_3$. Influence of the structure of the molecule on its reactivity. *Appl. Catal. B* **2010**, *95*, 217–227. [CrossRef]

22.	Zhang, Z.; Jiang, Z.; Shangguan, W. Low-temperature catalysis for VOCs removal in technology and application: A state-of-the-art review. *Catal. Today* **2016**, *264*, 270–278. [CrossRef]

23.	Li, W.B.; Wang, J.X.; Gong, H. Catalytic combustion of VOCs on non-noble metal catalysts. *Catal. Today* **2009**, *148*, 81–87. [CrossRef]

24.	Bratan, V.; Vasile, A.; Chesler, P.; Hornoiu, C. Insights into the redox and structural properties of CoO$_x$ and MnO$_x$: Fundamental factors affecting the catalytic performance in the oxidation process of VOCs. *Catalysts* **2022**, *12*, 1134. [CrossRef]

25.	Guo, Y.; Wen, M.; Li, G.; An, T. Recent advances in VOC elimination by catalytic oxidation technology onto various nanoparticles catalysts: A critical review. *Appl. Catal. B-Environ.* **2021**, *281*, 119447. [CrossRef]

26.	Song, S.; Zhang, S.; Zhang, X.; Verma, P.; Wen, M. Advances in catalytic oxidation of volatile organic compounds over Pd-supported catalysts: Recent trends and challenges. *Front. Mater.* **2020**, *7*, 595667. [CrossRef]

27.	Yang, J.; Xue, Y.; Liu, Y.; Deng, J.; Jiang, X.; Chen, H.; Dai, H. Mesoporous cobalt monoxide-supported platinum nanoparticles: Superior catalysts for the oxidative removal of benzene. *J. Environ. Sci.* **2020**, *90*, 170–179. [CrossRef]

28.	Liu, G.; Tian, Y.; Zhang, B.; Wang, L.; Zhang, X. Catalytic combustion of VOC on sandwich-structured Pt@ZSM-5 nanosheets prepared by controllable intercalation. *J. Hazard. Mater.* **2019**, *367*, 568–576. [CrossRef]

29.	Ma, X.; Yu, X.; Ge, M. Highly efficient catalytic oxidation of benzene over Ag assisted Co$_3$O$_4$ catalysts. *Catal. Today* **2021**, *376*, 262–268. [CrossRef]

30.	Chen, Z.; Li, J.; Yang, P.; Cheng, Z.; Li, J.; Zuo, S. Ce-modified mesoporous γ-Al$_2$O$_3$ supported Pd-Pt nanoparticle catalysts and their structure-function relationship in complete benzene oxidation. *Chem. Eng. J.* **2019**, *356*, 255–261. [CrossRef]

31.	Shi, Y.; Wan, J.; Kong, F.; Wang, Y.; Zhou, R. Influence of Pt dispersibility and chemical states on catalytic performance of Pt/CeO$_2$-TiO$_2$ catalysts for VOCs low-temperature removal. *Colloid Surface A* **2022**, *652*, 129932. [CrossRef]

32.	Wang, J.; Shi, Y.; Kong, F.; Zhou, R. Low-temperature VOCs oxidation performance of Pt/zeolites catalysts with hierarchical pore structure. *J. Environ. Sci.* **2023**, *124*, 505–512. [CrossRef]

33.	Shi, Y.; Guo, X.; Wang, Y.; Kong, F.; Zhou, R. New insight into the design of highly dispersed Pt supported CeO$_2$–TiO$_2$ catalysts with superior activity for VOCs low-temperature removal. *Green Energy Environ.* **2022**, *in press*. [CrossRef]

34.	Shi, Y.; Wang, J.; Zhou, R. Pt-support interaction and nanoparticle size effect in Pt/CeO$_2$-TiO$_2$ catalysts for low temperature VOCs removal. *Chemosphere* **2021**, *265*, 129127. [CrossRef] [PubMed]

35.	An, N.; Wu, P.; Li, S.; Jia, M.; Zhang, W. Catalytic oxidation of formaldehyde over Pt/Fe$_2$O$_3$ catalysts prepared by different method. *Appl. Surf. Sci.* **2013**, *285*, 805–809. [CrossRef]

36.	Zhang, Q.; Su, W.; Ning, P.; Liu, X.; Wang, H.; Hu, J. Catalytic performance and mechanistic study of toluene combustion over the Pt-Pd-HMS catalyst. *Chem. Eng. Sci.* **2019**, *205*, 230–237. [CrossRef]

37.	Hou, Z.; Zhou, X.; Lin, T.; Chen, Y.; Lai, X.; Feng, J.; Sun, M. The promotion effect of tungsten on monolith Pt/Ce$_{0.65}$Zr$_{0.35}$O$_2$ catalysts for the catalytic oxidation of toluene. *New J. Chem.* **2019**, *43*, 5719–5726. [CrossRef]

38.	Li, K.; Chen, J.; Bai, B.; Zhao, S.; Hu, F.; Li, J. Bridging the reaction route of toluene total oxidation and the structure of ordered mesoporous Co$_3$O$_4$: The roles of surface sodium and adsorbed oxygen. *Catal. Today* **2017**, *297*, 173–181. [CrossRef]

39.	Chang, S.; Jia, Y.; Zeng, Y.; Qian, F.; Guo, L.; Wu, S.; Lu, J.; Han, Y. Effect of interaction between different CeO$_2$ plane and platinum nanoparticles on catalytic activity of Pt/CeO$_2$ in toluene oxidation. *J. Rare Earth* **2021**, *40*, 1743–1750. [CrossRef]

40.	Wen, M.; Dong, F.; Yao, J.; Tang, Z.; Zhang, J. Pt nanoparticles confined in the ordered mesoporous CeO$_2$ as a highly efficient catalyst for the elimination of VOCs. *J. Catal.* **2022**, *412*, 42–58. [CrossRef]

41.	Wang, Z.; Yang, H.; Liu, R.; Xie, S.; Liu, Y.; Dai, H.; Huang, H.; Deng, J. Probing toluene catalytic removal mechanism over supported Pt nano- and single-atom-catalyst. *J. Hazard. Mater.* **2020**, *392*, 122258. [CrossRef] [PubMed]

42.	Wang, Z.; Ma, P.; Zheng, K.; Wang, C.; Liu, Y.; Dai, H.; Wang, C.; Hsi, H.-C.; Deng, J. Size effect, mutual inhibition and oxidation mechanism of the catalytic removal of a toluene and acetone mixture over TiO$_2$ nanosheet-supported Pt nanocatalysts. *Appl. Catal. B-Environ.* **2020**, *274*, 118963. [CrossRef]

43.	Ye, J.; Cheng, B.; Yu, J.; Ho, W.; Wageh, S.; Al-Ghamdi, A.A. Hierarchical Co$_3$O$_4$-NiO hollow dodecahedron-supported Pt for room-temperature catalytic formaldehyde decomposition. *Chem. Eng. J.* **2022**, *430*, 132715. [CrossRef]

44.	Zhang, C.; He, H. A comparative study of TiO$_2$ supported noble metal catalysts for the oxidation of formaldehyde at room temperature. *Catal. Today* **2007**, *126*, 345–350. [CrossRef]

45.	Kondratowicz, T.; Drozdek, M.; Michalik, M.; Gac, W.; Gajewska, M.; Kuśtrowski, P. Catalytic activity of Pt species variously dispersed on hollow ZrO$_2$ spheres in combustion of volatile organic compounds. *Appl. Surf. Sci.* **2020**, *513*, 145788. [CrossRef]

46.	An, N.; Zhang, W.; Yuan, X.; Pan, B.; Liu, G.; Jia, M.; Yan, W.; Zhang, W. Catalytic oxidation of formaldehyde over different silica supported platinum catalysts. *Chem. Eng. J.* **2013**, *215–216*, 1–6. [CrossRef]

47.	Kim, J.-M.; Vikrant, K.; Kim, T.; Kim, K.-H.; Dong, F. Thermocatalytic oxidation of gaseous benzene by a titanium dioxide supported platinum catalyst. *Chem. Eng. J.* **2022**, *428*, 131090. [CrossRef]

48.	Peng, R.; Sun, X.; Li, S.; Chen, L.; Fu, M.; Wu, J.; Ye, D. Shape effect of Pt/CeO$_2$ catalysts on the catalytic oxidation of toluene. *Chem. Eng. J.* **2016**, *306*, 1234–1246. [CrossRef]

49.	Avila, M.S.; Vignatti, C.I.; Apesteguía, C.R.; Garetto, T.F. Effect of support on the deep oxidation of propane and propylene on Pt-based catalysts. *Chem. Eng. J.* **2014**, *241*, 52–59. [CrossRef]

50.	Chen, Z.; Mao, J.; Zhou, R. Preparation of size-controlled Pt supported on Al$_2$O$_3$ nanocatalysts for deep catalytic oxidation of benzene at lower temperature. *Appl. Surf. Sci.* **2019**, *465*, 15–22. [CrossRef]

51.	Gao, W.; Tang, X.; Yi, H.; Jiang, S.; Yu, Q.; Xie, X.; Zhuang, R. Mesoporous molecular sieve-based materials for catalytic oxidation of VOC: A review. *J. Environ. Sci.* **2023**, *125*, 112–134. [CrossRef] [PubMed]

52.	Chang, M.; Liu, X.; Ning, P.; Zhang, Q.; Xia, F.; Wang, H.; Wei, G.; Wen, J.; Liu, M.; Hu, J.; et al. Removal of toluene over bi-metallic Pt–Pd-SBA-15 catalysts: Kinetic and mechanistic study. *Micropor. Mesopor. Mat.* **2020**, *302*, 110111. [CrossRef]

53.	Chen, D.; Qu, Z.; Sun, Y.; Gao, K.; Wang, Y. Identification of reaction intermediates and mechanism responsible for highly active HCHO oxidation on Ag/MCM-41 catalysts. *Appl. Catal. B-Environ.* **2013**, *142–143*, 838–848. [CrossRef]

54.	Chen, X.J.; Chen, F.; Lv, P.P.; Zhang, D.; Ding, G.L.; Hu, X.L.; Feng, C.; Sheng, J.Z.; Huang, H.F. Maternal high estradiol exposure alters CDKN1C and IGF2 expression in human placenta. *Placenta* **2018**, *61*, 72–79. [CrossRef]

55.	El Khawaja, R.; Sonar, S.; Barakat, T.; Heymans, N.; Su, B.-L.; Löfberg, A.; Lamonier, J.-F.; Giraudon, J.-M.; De Weireld, G.; Poupin, C.; et al. VOCs catalytic removal over hierarchical porous zeolite NaY supporting Pt or Pd nanoparticles. *Catal. Today* **2022**, *405–406*, 212–220. [CrossRef]

56.	Huang, H.; Hu, P.; Huang, H.; Chen, J.; Ye, X.; Leung, D.Y.C. Highly dispersed and active supported Pt nanoparticles for gaseous formaldehyde oxidation: Influence of particle size. *Chem. Eng. J.* **2014**, *252*, 320–326. [CrossRef]

57.	Wei, M.; Wu, S.; Mao, Q.; Wang, Y.; Guo, G.; Zhang, D. The oxidation mechanism investigation of benzene catalyzed by palladium nanoparticle: A ReaxFF molecular dynamics. *Fuel* **2020**, *275*, 117989. [CrossRef]

58.	Aguirre, A.; Fornero, E.L.; Villarreal, A.; Collins, S.E. Identification of key reaction intermediates during toluene combustion on a Pd/CeO$_2$ catalyst using operando modulated DRIFT spectroscopy. *Catal. Today* **2022**, *394–396*, 225–234. [CrossRef]

59.	Hong, J.; Chu, W.; Chen, M.; Wang, X.; Zhang, T. Preparation of novel titania supported palladium catalysts for selective hydrogenation of acetylene to ethylene. *Catal. Commun.* **2007**, *8*, 593–597. [CrossRef]

60.	He, C.; Li, J.; Zhang, X.; Yin, L.; Chen, J.; Gao, S. Highly active Pd-based catalysts with hierarchical pore structure for toluene oxidation: Catalyst property and reaction determining factor. *Chem. Eng. J.* **2012**, *180*, 46–56. [CrossRef]

61.	Wu, L.; Deng, J.; Liu, Y.; Jing, L.; Yu, X.; Zhang, X.; Gao, R.; Pei, W.; Hao, X.; Rastegarpanah, A.; et al. Pd/silicalite-1: An highly active catalyst for the oxidative removal of toluene. *J. Environ. Sci.* **2022**, *116*, 209–219. [CrossRef] [PubMed]

62.	Li, N.; Cheng, J.; Xing, X.; Sun, Y.; Hao, Z. Distribution and formation mechanisms of polychlorinated organic by-products upon the catalytic oxidation of 1,2-dichlorobenzene with palladium-loaded catalysts. *J. Hazard. Mater.* **2020**, *393*, 122412. [CrossRef] [PubMed]

63.	Aristizábal, B.H.; de Correa, C.M.; Serykh, A.I.; Hetrick, C.E.; Amiridis, M.D. In situ FTIR study of the adsorption and reaction of ortho-dichlorobenzene over Pd-promoted Co-HMOR. *Micropor. Mesopor. Mater.* **2008**, *112*, 432–440. [CrossRef]

64.	Aranzabal, A.; Romero-Sáez, M.; Elizundia, U.; González-Velasco, J.R.; González-Marcos, J.A. Deactivation of H-zeolites during catalytic oxidation of trichloroethylene. *J. Catal.* **2012**, *296*, 165–174. [CrossRef]

65.	Sun, P.; Wang, W.; Dai, X.; Weng, X.; Wu, Z. Mechanism study on catalytic oxidation of chlorobenzene over Mn$_x$ Ce$_{1-x}$O$_2$/ H-ZSM5 catalysts under dry and humid conditions. *Appl. Catal. B-Environ.* **2016**, *198*, 389–397. [CrossRef]

66.	Jabłońska, M.; Król, A.; Kukulska-Zając, E.; Tarach, K.; Girman, V.; Chmielarz, L.; Góra-Marek, K. Zeolites Y modified with palladium as effective catalysts for low-temperature methanol incineration. *Appl. Catal. B-Environ.* **2015**, *166–167*, 353–365. [CrossRef]

67.	He, C.; Zhang, F.; Yue, L.; Shang, X.; Chen, J.; Hao, Z. Nanometric palladium confined in mesoporous silica as efficient catalysts for toluene oxidation at low temperature. *Appl. Catal. B-Environ.* **2012**, *111–112*, 46–57. [CrossRef]

68.	Deng, H.; Kang, S.; Wang, C.; He, H.; Zhang, C. Palladium supported on low-surface-area fiber-based materials for catalytic oxidation of volatile organic compounds. *Chem. Eng. J.* **2018**, *348*, 361–369. [CrossRef]

69.	Yue, L.; He, C.; Hao, Z.; Wang, S.; Wang, H. Effects of metal and acidic sites on the reaction by-products of butyl acetate oxidation over palladium-based catalysts. *J. Environ. Sci.* **2014**, *26*, 702–707. [CrossRef]

70.	Yi, H.; Miao, L.; Xu, J.; Zhao, S.; Xie, X.; Du, C.; Tang, T.; Tang, X. Palladium particles supported on porous CeMnO$_3$ perovskite for catalytic oxidation of benzene. *Colloid Surface A* **2021**, *623*, 126687. [CrossRef]

71.	He, J.; Zheng, F.; Zhou, Y.; Li, X.; Wang, Y.; Xiao, J.; Li, Y.; Chen, D.; Lu, J. Catalytic oxidation of VOCs over 3D@2D Pd/CoMn$_2$O$_4$ nanosheets supported on hollow Al$_2$O$_3$ microspheres. *J. Colloid Interface Sci.* **2022**, *613*, 155–167. [CrossRef] [PubMed]

72.	Xu, C.; Fang, R.; Luque, R.; Chen, L.; Li, Y. Functional metal–organic frameworks for catalytic applications. *Coordin Chem. Rev.* **2019**, *388*, 268–292. [CrossRef]

73.	Li, J.; Xu, Z.; Wang, T.; Xie, X.; Li, D.; Wang, J.; Huang, H.; Ao, Z. A versatile route to fabricate Metal/UiO-66 (Metal = Pt, Pd, Ru) with high activity and stability for the catalytic oxidation of various volatile organic compounds. *Chem. Eng. J.* **2022**, *448*, 136900. [CrossRef]

74.	Hou, Z.; Pei, W.; Zhang, X.; Zhang, K.; Liu, Y.; Deng, J.; Jing, L.; Dai, H. Rare earth oxides and their supported noble metals in application of environmental catalysis. *J. Rare Earth* **2020**, *38*, 819–839. [CrossRef]

75. Yan, H.; Zhang, N.; Wang, D. Highly efficient CeO$_2$-supported noble-metal catalysts: From single atoms to nanoclusters. *Chem. Catal.* **2022**, *2*, 1594–1623. [CrossRef]

76. Gil, S.; Garcia-Vargas, J.; Liotta, L.; Pantaleo, G.; Ousmane, M.; Retailleau, L.; Giroir-Fendler, A. Catalytic oxidation of propene over Pd catalysts supported on CeO$_2$, TiO$_2$, Al$_2$O$_3$ and M/Al$_2$O$_3$ oxides (M = Ce, Ti, Fe, Mn). *Catalysts* **2015**, *5*, 671–689. [CrossRef]

77. Zhao, Q.; Ge, Y.; Fu, K.; Zheng, Y.; Liu, Q.; Song, C.; Ji, N.; Ma, D. Catalytic performance of the Pd/TiO$_2$ modified with MnOx catalyst for acetone total oxidation. *Appl. Surf. Sci.* **2019**, *496*, 143579. [CrossRef]

78. Taylor, M.; Ndifor, E.N.; Garcia, T.; Solsona, B.; Carley, A.F.; Taylor, S.H. Deep oxidation of propane using palladium–titania catalysts modified by niobium. *Appl. Catal. A-Gen.* **2008**, *350*, 63–70. [CrossRef]

79. Aznárez, A.; Korili, S.A.; Gil, A. The promoting effect of cerium on the characteristics and catalytic performance of palladium supported on alumina pillared clays for the combustion of propene. *Appl. Catal. A-Gen.* **2014**, *474*, 95–99. [CrossRef]

80. He, Z.; He, Z.; Wang, D.; Bo, Q.; Fan, T.; Jiang, Y. Mo-modified Pd/Al$_2$O$_3$ catalysts for benzene catalytic combustion. *J. Environ. Sci.* **2014**, *26*, 1481–1487. [CrossRef]

81. Solsona, B.; Aylon, E.; Murillo, R.; Mastral, A.M.; Monzonis, A.; Agouram, S.; Davies, T.E.; Taylor, S.H.; Garcia, T. Deep oxidation of pollutants using gold deposited on a high surface area cobalt oxide prepared by a nanocasting route. *J. Hazard. Mater.* **2011**, *187*, 544–552. [CrossRef]

82. Liu, Y.; Dai, H.; Deng, J.; Xie, S.; Yang, H.; Tan, W.; Han, W.; Jiang, Y.; Guo, G. Mesoporous Co$_3$O$_4$-supported gold nanocatalysts: Highly active for the oxidation of carbon monoxide, benzene, toluene, and o-xylene. *J. Catal.* **2014**, *309*, 408–418. [CrossRef]

83. Solsona, B.; Garcia, T.; Aylón, E.; Dejoz, A.M.; Vázquez, I.; Agouram, S.; Davies, T.E.; Taylor, S.H. Promoting the activity and selectivity of high surface area Ni–Ce–O mixed oxides by gold deposition for VOC catalytic combustion. *Chem. Eng. J.* **2011**, *175*, 271–278. [CrossRef]

84. Grisel, R.J.H.; Kooyman, P.J.; Nieuwenhuys, B.E. Influence of the Preparation of Au/Al$_2$O$_3$ on CH$_4$ Oxidation Activity. *J. Catal.* **2000**, *191*, 430–437. [CrossRef]

85. Bond, G.C.; Thompson, D.T. Catalysis by Gold. *Catal. Rev.* **1999**, *41*, 319–388. [CrossRef]

86. Solsona, B.; Garcia, T.; Jones, C.; Taylor, S.; Carley, A.; Hutchings, G. Supported gold catalysts for the total oxidation of alkanes and carbon monoxide. *Appl. Catal. A-Gen.* **2006**, *312*, 67–76. [CrossRef]

87. Jia, M.; Shen, Y.; Li, C.; Bao, Z.; Sheng, S. Effect of supports on the gold catalyst activity for catalytic combustion of CO and HCHO. *Catal. Lett.* **2005**, *99*, 235–239. [CrossRef]

88. Shen, Y.; Yang, X.; Wang, Y.; Zhang, Y.; Zhu, H.; Gao, L.; Jia, M. The states of gold species in CeO$_2$ supported gold catalyst for formaldehyde oxidation. *Appl. Catal. B-Environ.* **2008**, *79*, 142–148. [CrossRef]

89. Hosseini, M.; Siffert, S.; Tidahy, H.L.; Cousin, R.; Lamonier, J.F.; Aboukais, A.; Vantomme, A.; Roussel, M.; Su, B.L. Promotional effect of gold added to palladium supported on a new mesoporous TiO$_2$ for total oxidation of volatile organic compounds. *Catal. Today* **2007**, *122*, 391–396. [CrossRef]

90. Xu, J.; Qu, Z.; Ke, G.; Wang, Y.; Huang, B. Catalytic activity of gold-silver nanoalloys for HCHO oxidation: Effect of hydroxyl and particle size. *Appl. Surf. Sci.* **2020**, *513*, 145910. [CrossRef]

91. Hosseini, M.; Barakat, T.; Cousin, R.; Aboukaïs, A.; Su, B.L.; De Weireld, G.; Siffert, S. Catalytic performance of core–shell and alloy Pd–Au nanoparticles for total oxidation of VOC: The effect of metal deposition. *Appl. Catal. B-Environ.* **2012**, *111–112*, 218–224. [CrossRef]

92. Zhao, B.; Jin, B.; Wu, X.; Weng, D.; Ran, R. Ag-modified SmMn$_2$O$_5$ catalysts for CO and C$_3$H$_8$ oxidation. *Catal. Commun.* **2022**, *167*, 106456. [CrossRef]

93. Wang, Y.; Bi, F.; Wang, Y.; Jia, M.; Tao, X.; Jin, Y.; Zhang, X. MOF-derived CeO$_2$ supported Ag catalysts for toluene oxidation: The effect of synthesis method. *Mol. Catal.* **2021**, *515*, 111922. [CrossRef]

94. Dong, N.; Ye, Q.; Zhang, D.; Xiao, Y.; Dai, H. Reduced graphene oxide as an effective promoter to the layered manganese oxide-supported Ag catalysts for the oxidation of ethyl acetate and carbon monoxide. *J. Hazard. Mater.* **2022**, *431*, 128518. [CrossRef] [PubMed]

95. Benaissa, S.; Cherif-Aouali, L.; Hany, S.; Labaki, M.; Aouad, S.; Cousin, R.; Siffert, S.; Aboukaïs, A. Influence of the preparation method and silver content on the nature of active sites in Ag/CeO$_2$ catalysts used for propylene oxidation. *Chem. Phys.* **2022**, *558*, 111499. [CrossRef]

96. Bhat, A.; Hill, A.J.; Fisher, G.B.; Schwank, J.W. Improving the thermal stability and n-butanol oxidation activity of Ag-TiO$_2$ catalysts by controlling the catalyst architecture and reaction conditions. *Appl. Catal. B-Environ.* **2021**, *297*, 120476. [CrossRef]

97. Tang, X.; Feng, F.; Ye, L.; Zhang, X.; Huang, Y.; Liu, Z.; Yan, K. Removal of dilute VOCs in air by post-plasma catalysis over Ag-based composite oxide catalysts. *Catal. Today* **2013**, *211*, 39–43. [CrossRef]

98. Wynblatt, P.; Gjostein, N. Supported metal crystallites. *Prog. Solid State Chem.* **1975**, *9*, 21–58. [CrossRef]

99. Schick, L.; Sanchis, R.; González-Alfaro, V.; Agouram, S.; López, J.M.; Torrente-Murciano, L.; García, T.; Solsona, B. Size-activity relationship of iridium particles supported on silica for the total oxidation of volatile organic compounds (VOCs). *Chem. Eng. J.* **2019**, *366*, 100–111. [CrossRef]

100. Wang, Z.; Zhang, L.; Ji, J.; Wu, Y.; Cai, Y.; Yao, X.; Gu, X.; Xiong, Y.; Wan, H.; Dong, L.; et al. Catalytic enhancement of small sizes of CeO$_2$ additives on Ir/Al$_2$O$_3$ for toluene oxidation. *Appl. Surf. Sci* **2022**, *571*, 151200. [CrossRef]